photonics

MDPI

Article

Multi-Mode Correlation in a Concurrent Parametric Amplifier

Hailong Wang * and Yunpeng Shi

College of Optical and Electronic Technology, China Jiliang University, Hangzhou 310018, China; p21040854081@cjlu.edu.cn
* Correspondence: hlwang@cjlu.edu.cn

Abstract: A concurrent parametric amplifier consisting of two pump beams is used to investigate the possibility of generating multi-mode correlation and entanglement. The existence of three-mode entanglement is demonstrated by analyzing the violation degree of three-mode entanglement criteria, including the sufficient criterion, i.e., two-condition and optimal single-condition criterion, and necessary and sufficient criterion, i.e., positivity under partial transposition (PPT) criterion. Besides, two-mode entanglement generated from any pair is also studied by using the Duan criterion and PPT criterion. We find that three-mode entanglement and two-mode entanglement of the two pairs are present in the whole parameter region. Our results pave the way for the realization and application of multi-mode correlation and entanglement based on the concurrent parametric amplifiers.

Keywords: multi-mode correlation; concurrent; parametric amplifier

check for updates

Citation: Wang, H.; Shi, Y. Multi-Mode Correlation in a Concurrent Parametric Amplifier. *Photonics* **2022**, *9*, 443. https://doi.org/10.3390/photonics9070443

Received: 24 May 2022
Accepted: 20 June 2022
Published: 23 June 2022

1. Introduction

Parametric amplifier, for example, four-wave mixing (FWM), acts as a nonlinear interaction process that permits the transfer of energy and momentum between multiple optical modes, specifically, two pump modes can be converted into a signal and an idler modes via various nonlinear media [1–3]. For the atomic medium, a high-power pump beam intersects a low-power seed beam in a hot rubidium cell, causing them to interact and generate an idler beam, then the amplified seed (signal) and the newly-generated idler beams can be demonstrated to be quantum correlated and entangled [4–10]. Based on this simple model of only one pump mode and only one seed mode, other variations have been presented. For example, when the FWM process is seeded by the coherent signal and idler beams and only pumped by one pump beam, a scheme of a two-mode phase-sensitive amplifier has been constructed, and its classical and quantum properties have been theoretically analyzed [11] and experimentally measured [12]. Similarly, when the FWM process is seeded by two coherent signal beams at the same angle but in opposite directions on either side of the pump beam, this dual-seed scheme has been allowed to achieve intensity-difference squeezing at ultra-low frequency [13].

On the other hand, with the FWM process pumped by two coherent pump beams with non-degenerate frequency and only seeded by one coherent signal beam, a noiseless optical amplifier has been experimentally realized, and its noise figure is always superior than that obtained with a phase-insensitive amplifier with the same gain [14].

Motivated by the above scientific advances, we propose a concurrent parametric amplifier scheme in which FWM process is pumped by the two coherent pump beams with the degenerate frequency and only seeded by one coherent signal beam. As shown in Figure 1, two pump beams P_1 and P_2 are focused and crossed in the center of a hot rubidium vapor cell. A coherent seed beam, red-shifted from pump beam as shown in the block in Figure 1, is seeded into the vapor cell, and it symmetrically crosses with the two pump beams on one plane with the proper crossing angles [15] to eliminate any other cascaded FWM processes. Under this experimental condition, each pump beam will interact with the seed beam individually by means of FWM process. The seed beam is amplified

(S) and two idler beams (I_1 and I_2) are simultaneously generated, therefore the interaction mechanism of the triple output beams S, I_1 and I_2 constitute a concurrent parametric amplification process [16]. In this work, the quantum properties of two-mode and three-mode entanglement existed in the triple output beams generated from the concurrent parametric amplifier will be discussed in detail. Firstly, the Hamiltonian describing this concurrent parametric amplifier can be written as below

$$\hat{H} = i\hbar[\varepsilon_1(\hat{a}_s^\dagger \hat{a}_1^\dagger - \hat{a}_s \hat{a}_1) + \varepsilon_2(\hat{a}_s^\dagger \hat{a}_2^\dagger - \hat{a}_s \hat{a}_2)], \tag{1}$$

with ε_i (i = 1 and 2) representing the interaction strength and $\hat{a}_i$ (i = s, 1, and 2) the bosonic annihilation operators. By applying the Heisenberg equation of motion to Equation (1), the solution for the annihilation operators is found to be

$$\begin{aligned} \hat{a}_s(t) &= A\hat{a}_s(0) + B\hat{a}_1^\dagger(0) + C\hat{a}_2^\dagger(0), \\ \hat{a}_1(t) &= B\hat{a}_s^\dagger(0) + D\hat{a}_1(0) + E\hat{a}_2(0), \\ \hat{a}_2(t) &= C\hat{a}_s^\dagger(0) + Ea_1(0) + F\hat{a}_2(0), \end{aligned} \tag{2}$$

with

$$\begin{aligned} A &= \sqrt{G}, \\ B &= \tfrac{\alpha\sqrt{G-1}}{\sqrt{1+\alpha^2}}, \\ C &= \tfrac{\sqrt{G-1}}{\sqrt{1+\alpha^2}}, \\ D &= \tfrac{1+\alpha^2\sqrt{G}}{1+\alpha^2}, \\ E &= \tfrac{\alpha(\sqrt{G}-1)}{1+\alpha^2}, \\ F &= \tfrac{\alpha^2+\sqrt{G}}{1+\alpha^2}, \end{aligned} \tag{3}$$

where $\Gamma = \sqrt{\varepsilon_1^2 + \varepsilon_2^2}$, $\cosh(\Gamma t) = \sqrt{G}$, and $\varepsilon_1/\varepsilon_2 = \alpha$. Before investigating the two-mode and three-mode entanglement existing in the system, the optical quadrature definitions should be given firstly due to the requirement of the following criteria. Concerning the three modes characterized by bosonic annihilation operators $\hat{a}_i$ involved in the present system, where i = s, 1, and 2, quadrature operators can be defined as follows:

$$X_i = \hat{a}_i + \hat{a}_i^\dagger, Y_i = -i(\hat{a}_i - \hat{a}_i^\dagger), \tag{4}$$

such that $[X_i, Y_i]$ = $2i$, and X_i and Y_i are, respectively, position and momentum quadratures. Following the definitions of Equation (4), Equation (2) can be recast in the form of quadrature operators:

$$\begin{aligned} X_s(t) &= AX_s(0) + BX_1(0) + CX_2(0), \\ X_1(t) &= BX_s(0) + DX_1(0) + EX_2(0), \\ X_2(t) &= CX_s(0) + EX_1(0) + FX_2(0), \end{aligned} \tag{5}$$

and

$$\begin{aligned} Y_s(t) &= AY_s(0) - BY_1(0) - CY_2(0), \\ Y_1(t) &= -BY_s(0) + DY_1(0) + EY_2(0), \\ Y_2(t) &= -CY_s(0) + EY_1(0) + FY_2(0). \end{aligned} \tag{6}$$

Based on the above relations about quadrature operators, the variances and covariances of the position and momentum quadratures can be obtained to analyze the violation degree of different entanglement criteria. $V(X_i) = \langle X_i^2 \rangle - \langle X_i \rangle^2$ represents the position quadrature

variance. For the covariance, it can be defined as $V_{ij} = (\langle X_i X_j \rangle + \langle X_j X_i \rangle)/2 - \langle X_i \rangle \langle X_j \rangle$. It should be noted that the covariance V_{ij} will reduce to the usual variance $V(X_i)$ under the condition of $i = j$. In reality, the variances of the three modes can be expressed as

$$\begin{aligned} \left\langle X_s^2(t) \right\rangle &= \langle Y_s^2(t) \rangle = A^2 + B^2 + C^2 = 2G - 1, \\ \left\langle X_1^2(t) \right\rangle &= \langle Y_1^2(t) \rangle = B^2 + D^2 + E^2 = \tfrac{1+\alpha^2(2G-1)}{1+\alpha^2}, \\ \left\langle X_2^2(t) \right\rangle &= \langle Y_2^2(t) \rangle = C^2 + E^2 + F^2 = \tfrac{\alpha^2+(2G-1)}{1+\alpha^2}, \end{aligned} \tag{7}$$

and here, we used the fact that the mean values of quadrature operators are all equal to 0 and $\langle X_i(0) X_j(0) \rangle = \langle Y_i(0) Y_j(0) \rangle = \delta_{ij}$ (i, j = s, 1, and 2). Similarly, the covariances can be expressed by

$$\begin{aligned} \langle X_s(t) X_1(t) \rangle &= -\langle Y_s(t) Y_1(t) \rangle = AB + BD + CE \\ &= \tfrac{2\alpha\sqrt{G(G-1)}}{\sqrt{1+\alpha^2}}, \\ \langle X_s(t) X_2(t) \rangle &= -\langle Y_s(t) Y_2(t) \rangle = AC + BE + CF \\ &= \tfrac{2\sqrt{G(G-1)}}{\sqrt{1+\alpha^2}}, \\ \langle X_1(t) X_2(t) \rangle &= \langle Y_1(t) Y_2(t) \rangle = BC + DE + EF \\ &= \tfrac{2\alpha(G-1)}{1+\alpha^2}, \end{aligned} \tag{8}$$

and the above expressions can be used to discuss the entanglement properties of both two-mode and three-mode cases; this is due to the fact that the triple beams in the concurrent parametric amplifier are Gaussian states, which can be fully quantified by their corresponding covariance matrix (CM).

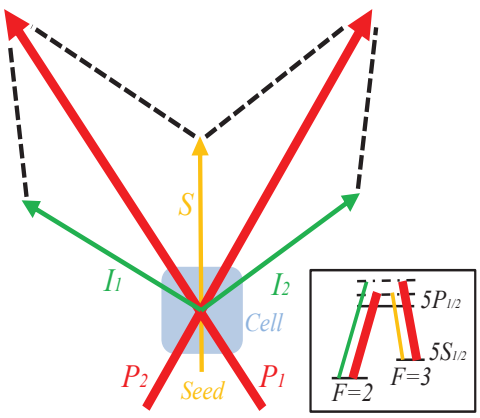

Figure 1. The concurrent parametric amplifier. P_1 and P_2: two pump beams; S: signal beam; I_1 and I_2: two idler beams. The energy level is shown in the block.

2. Two-Mode Entanglement

2.1. Duan Criterion

On the one hand, two-mode entanglement in this concurrent parametric amplifier is analyzed using a sufficient criterion, i.e., Duan criterion [17], which is based on the total variance of a pair of Einstein–Podolsky–Rosen-type operators, $X_i - X_j$ and $Y_i + Y_j$. For physical entangled continuous variable states, this variance will rapidly reduce to zero by increasing the correlation degree. Thus, if any inequality in Equation (9) is violated, there will exist two-mode entanglement between any pair. Based on the quadrature definitions in Equation (4), the inequalities can be expressed asnumerical order.

$$\begin{aligned} D_{s1} &= V(X_s - X_1) + V(Y_s + Y_1) \geq 4, \\ D_{s2} &= V(X_s - X_2) + V(Y_s + Y_2) \geq 4, \\ D_{12} &= V(X_1 - X_2) + V(Y_1 + Y_2) \geq 4. \end{aligned} \tag{9}$$

We calculate the dependence of D_{s1}, D_{s2}, and D_{12} on the gain G and interaction strength ratio α as

$$\begin{aligned} D_{s1} &= 2[2G - 1 - \frac{4\alpha\sqrt{G(G-1)}}{\sqrt{1+\alpha^2}} + \frac{1+\alpha^2(2G-1)}{1+\alpha^2}], \\ D_{s2} &= 4[G - \frac{2\sqrt{G(G-1)}}{\sqrt{1+\alpha^2}} + \frac{G-1}{1+\alpha^2}], \\ D_{12} &= 4G. \end{aligned} \tag{10}$$

The violation of the first, second, and third inequalities in Equation (9) can be used to claim the existence of two-mode entanglement between $\hat{a}_s$ and $\hat{a}_1$, $\hat{a}_s$ and $\hat{a}_2$, and $\hat{a}_1$ and $\hat{a}_2$, respectively. As depicted in Figure 2a, as G and α get larger, the value of D_{s1} becomes smaller and smaller. This is because, under this condition, the concurrent parametric amplifier will reduce to a simple single pump amplifier only pumped by P_1, and two-mode entanglement between the modes $\hat{a}_s$ and $\hat{a}_1$ will dominate. Contrary to the dependence of D_{s1} on G and α, the two-mode entanglement between $\hat{a}_s$ and $\hat{a}_2$ depicted in Figure 2b can be improved by means of a larger value of G and a smaller value of α, meaning that, in this situation, the concurrent parametric amplifier will reduce to the simple single-pump amplifier only pumped by P_2, and two-mode entanglement between the modes $\hat{a}_s$ and $\hat{a}_2$ will dominate. This also explains the opposite behaviors between Figure 2a,b. More interestingly, as depicted in Figure 2c, two-mode entanglement between $\hat{a}_1$ and $\hat{a}_2$ is absent. The reason for this phenomenon is that the two modes $\hat{a}_1$ and $\hat{a}_2$ are both generated from the seed mode $\hat{a}_s$ and compete with each other.

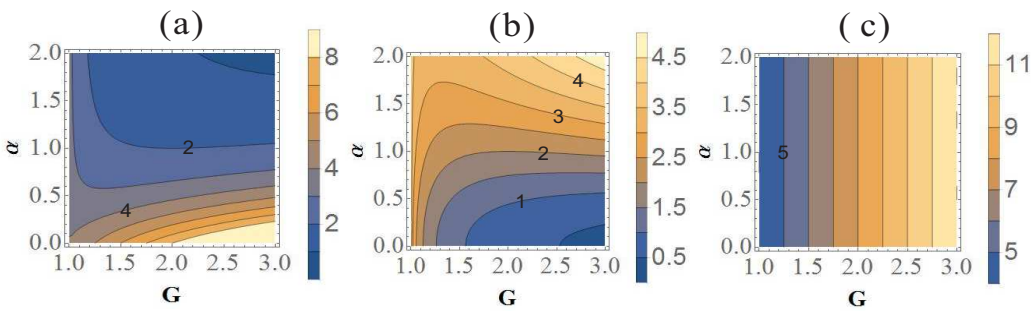

Figure 2. The dependence of D_{s1} (**a**), D_{s2} (**b**), and D_{12} (**c**) on the gain G and interaction strength ratio α.

2.2. Positivity under Partial Transposition Criterion

On the other hand, the PPT criterion as a necessary and sufficient criterion can be used to quantify two-mode entanglement in the concurrent parametric amplifier. Generally, two-mode entanglement shared by $\hat{a}_s$ and $\hat{a}_1$ can be fully quantified by the following CM_{s1} [18,19]:

$$CM_{s1} = \begin{bmatrix} \langle \hat{X}_s^2(t) \rangle & 0 & \langle \hat{X}_s(t)\hat{X}_1(t) \rangle & 0 \\ 0 & \langle \hat{Y}_s^2(t) \rangle & 0 & \langle \hat{Y}_s(t)\hat{Y}_1(t) \rangle \\ \langle \hat{X}_s(t)\hat{X}_1(t) \rangle & 0 & \langle \hat{X}_1^2(t) \rangle & 0 \\ 0 & \langle \hat{Y}_s(t)\hat{Y}_1(t) \rangle & 0 & \langle \hat{Y}_1^2(t) \rangle \end{bmatrix}. \tag{11}$$

Only when both of the symplectic eigenvalues of the partially transposed (PT) CM_{s1} are no less than 1, this indicates the absence of two-mode entanglement between them [18–21].

In this way, the smaller symplectic eigenvalue E_{s1} can be used to quantify two-mode entanglement between $\hat{a}_s$ and $\hat{a}_1$, i.e., if E_{s1} is smaller than 1, two-mode entanglement will exist between them. Substituting Equations (7) and (8) into Equation (11), we can obtain the detailed result for E_{s1} as below:

$$E_{s1} = \frac{1}{(1+\alpha^2)^{3/2}} \sqrt{\begin{array}{c} 1+\alpha^2+(1+\alpha^2)[\alpha^4+2(G+2G\alpha^2)^2-2G(1+3\alpha^2+4\alpha^4)]- \\ 2(1+\alpha^2)[G+(2G-1)\alpha^2]\sqrt{(G-1)[G(1+2\alpha^2)^2-1]} \end{array}}, \quad (12)$$

and the dependence of E_{s1} is depicted in Figure 3a. Due to the value of E_{s1} being smaller than 1, thus $\hat{a}_s$ is quantum entangled with $\hat{a}_1$ in the whole parametric region ($G > 1$ and $\alpha > 0$). Similarly, the smaller symplectic eigenvalue E_{s2} of $\hat{a}_s$ and $\hat{a}_2$ can be calculated as

$$E_{s2} = \frac{1}{(1+\alpha^2)^{3/2}} \sqrt{\begin{array}{c} 1+\alpha^2+(1+\alpha^2)[\alpha^4+2G^2(2+\alpha^2)^2-2G(4+3\alpha^2+\alpha^4)] \\ -2(1+\alpha^2)[G(2+\alpha^2)-1]\sqrt{(G-1)[G(2+\alpha^2)^2-\alpha^4]} \end{array}}, \quad (13)$$

and its value is smaller than 1 in the whole parametric region as depicted in Figure 3b, meaning that $\hat{a}_s$ is also quantum entangled with $\hat{a}_2$.

Besides, the smaller symplectic eigenvalue E_{12} of $\hat{a}_1$ and $\hat{a}_2$ can be given by

$$E_{12} = \frac{1-G-\alpha^2+G\alpha^2+\sqrt{G^2-4\alpha^2+8G\alpha^2-2G^2\alpha^2+G^2\alpha^4}}{1+\alpha^2}, \quad (14)$$

and its value is larger than 1 in the whole parametric region, as depicted in Figure 3c, indicating that $\hat{a}_1$ is not quantum entangled with $\hat{a}_2$. This is determined by the following fact: $\hat{a}_1$ and $\hat{a}_2$ are both generated from $\hat{a}_s$ and in a competitive relationship.

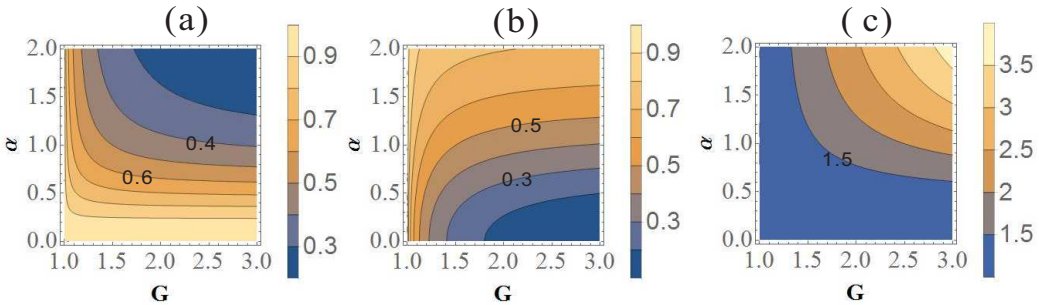

Figure 3. The dependence of E_{s1} (**a**), E_{s2} (**b**), and E_{12} (**c**) on the gain G and interaction strength ratio α.

3. Three-Mode Entanglement

3.1. Two-Condition Criterion

In the following, we analyze three-mode entanglement by using different criteria, i.e., two-condition, optimal single-condition, and PPT. First of all, a set of inequalities based on the two-condition criterion [22] is given by

$$\begin{aligned} V_{s1} &= V(X_s - X_1) + V(Y_s + Y_1 + O_2 Y_2) \geq 4, \\ V_{12} &= V(X_1 - X_2) + V(Y_1 + Y_2 + O_s Y_s) \geq 4, \end{aligned} \quad (15)$$

where O_i ($i = s, 2$), as arbitrary real numbers can be used to minimize the values in Equation (15). If the two inequalities in Equation (15) are both violated, then it can be deemed as a sufficient criterion to claim the presence of genuine three-mode entanglement. Following this idea, via direct differentiation of Equation (15) with regard to O_i, the optimal results of O_i (O_i^{opt}) can be given by

$$
\begin{aligned}
O_s &= \frac{-(\langle Y_s Y_1\rangle + \langle Y_s Y_2\rangle)}{\langle Y_s^2\rangle} \\
&= \frac{2\sqrt{G(G-1)}(1+\alpha)}{(2G-1)\sqrt{1+\alpha^2}}, \\
O_2 &= \frac{-(\langle Y_s Y_2\rangle + \langle Y_1 Y_2\rangle)}{\langle Y_2^2\rangle} \\
&= \frac{2[\alpha - G\alpha + \sqrt{G(G-1)(1+\alpha^2)}]}{2G-1+\alpha^2},
\end{aligned} \tag{16}
$$

and substituting Equation (16) into Equation (15), the detailed expression of Equation (15) can be expressed as

$$
\begin{aligned}
V_{s1} &= \frac{4(G+\alpha^2)[G+2G\alpha^2-\alpha(\alpha+2\sqrt{G(G-1)(1+\alpha^2)})]}{(1+\alpha^2)(2G-1+\alpha^2)}, \\
V_{12} &= \frac{4G[G(\alpha-1)^2+2\alpha]}{(1+\alpha^2)(2G-1)}.
\end{aligned} \tag{17}
$$

The contour plot of Equation (17) is shown in Figure 4. The dependence of V_{s1} on G and α is shown in Figure 4a. The region of $V_{s1} < 4$ is enlarged compared to the one of $D_{s1} < 4$ in Figure 2a when we consider the phase quadrature of $\hat{a}_2$ (Y_2). The variance of $Y_s + Y_1 + Y_2$ becomes smaller than the one of $Y_s + Y_1$, which claims that $\hat{a}_2$ has a correlation with $\hat{a}_s + \hat{a}_1$. The dependence of V_{12} on G and α is shown in Figure 4b, and the region of $V_{12} < 4$ is also enlarged compared to the one of $D_{12} < 4$ in Figure 2c due to the same reason.

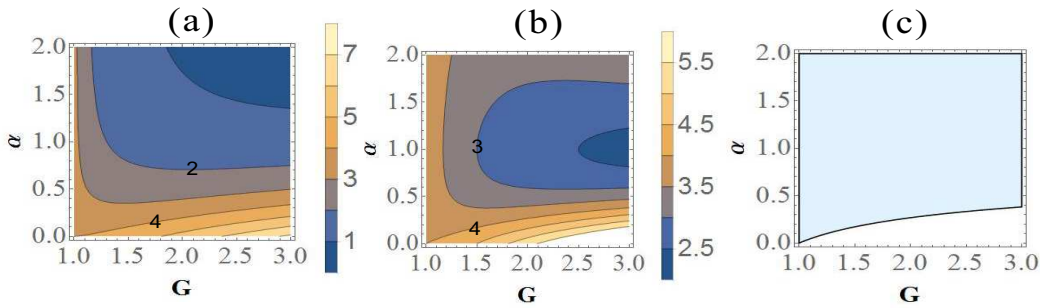

Figure 4. The contour plot of V_{s1} (**a**) and V_{12} (**b**); (**c**) the overlapped region between $V_{s1} < 4$ and $V_{12} < 4$.

The overlapped light blue region between $V_{s1} < 4$ and $V_{12} < 4$ in Figure 4c means that genuine three-mode entanglement is present in this system.

3.2. Optimal Single-Condition Criterion

Secondly, the single-condition criterion using the combined quadrature variances [22] can be used to test and verify the presence of genuine three-mode entanglement. If its value in Equation (18) is no more than 2, genuine three-mode entanglement can be verified.

$$
\begin{aligned}
V_{s12} &= V[X_s - \frac{1}{\sqrt{2}}(X_1+X_2)] + V[Y_s + \frac{1}{\sqrt{2}}(Y_1+Y_2)] \\
&= 2[3G-1+(G-1)\frac{2\alpha}{1+\alpha^2} - \frac{2(1+\alpha)\sqrt{2G(G-1)}}{\sqrt{1+\alpha^2}}].
\end{aligned} \tag{18}
$$

The dependence of V_{s12} is depicted in Figure 5, and its value in most of the region is no more than 2, which clearly shows the presence of genuine three-mode entanglement. Inspired by the above results, by introducing different factors [22] instead of $1/\sqrt{2}$, the noise unbalance between $\hat{a}_1$ and $\hat{a}_2$ in Equation (18) can be effectively canceled; this criterion

can be called the optimal single-condition criterion. In this way, V_{s12}^{opt} can be expressed as follows:

$$V_{s12}^{opt} = V[X_s - F_1X_1 - F_2X_2] + V[Y_s + F_1Y_1 + F_2Y_2], \tag{19}$$

where the optimal expressions (F_1^{opt} and F_2^{opt}) of F_1 and F_2 can be calculated as

$$\begin{aligned} F_1^{opt} &= \frac{2\alpha\sqrt{G(G-1)}}{(2G-1)\sqrt{1+\alpha^2}}, \\ F_2^{opt} &= \frac{2\sqrt{G(G-1)}}{(2G-1)\sqrt{1+\alpha^2}}, \end{aligned} \tag{20}$$

respectively. Substituting Equation (20) into Equation (19), V_{s12}^{opt} can be simply written as

$$V_{s12}^{opt} = \frac{2}{2G-1}. \tag{21}$$

The contour plot of V_{s12}^{opt} is depicted in Figure 6a, and it is not dependent on interaction strength ratio α, meaning that the generation of the two modes $\hat{a}_1$ and $\hat{a}_2$ is the mode X_s; thus, $F_1X_1 + F_2X_2$ is a combined idler mode with respect to the signal mode X_s.

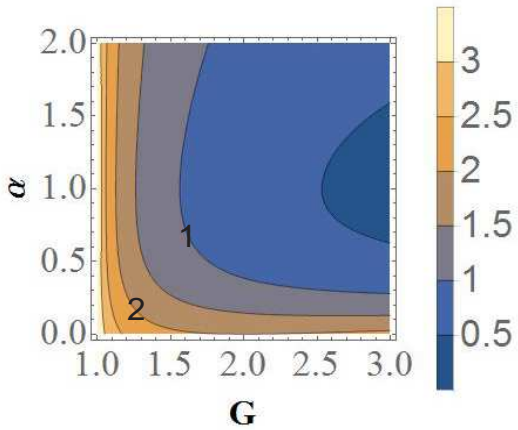

Figure 5. The dependence of V_{s12} in Equation (18).

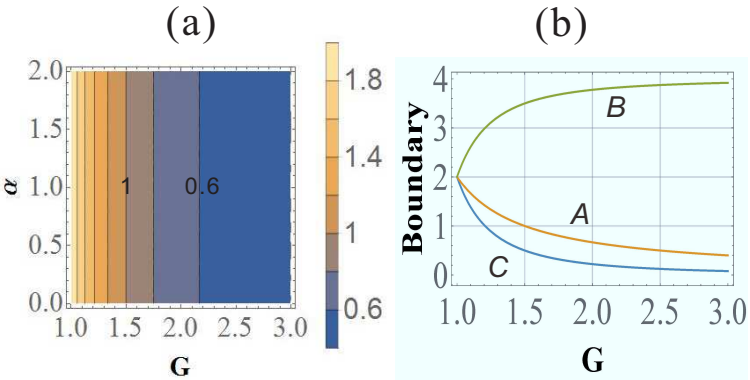

Figure 6. (**a**) The dependence of V_{s12}^{opt} in Equation (21); (**b**) the dependence of V_{s12}^{opt} (trace A); B_1 (trace B); $(B_2)_{\min} = (B_3)_{\min}$ (trace C).

To verify the presence of genuine three-mode entanglement, all the boundaries should be calculated according to [22]. If the value of Equation (21) is smaller than the smallest boundary, there will exist genuine three-mode entanglement. In this sense, the boundaries of V_{s12}^{opt} are $B_1 = 2(1 + |F_1^2 + F_2^2|)$, $B_2 = 2(|F_1^2| + |1 - F_2^2|)$, and $B_3 = 2(|F_2^2| + |1 - F_1^2|)$ with the detailed expressions of

$$\begin{aligned} B_1 &= 4 - \frac{2}{(2G-1)^2}, \\ B_2 &= \frac{2 + 2[1 + 8G(G-1)]\alpha^2}{(2G-1)^2(1+\alpha^2)}, \\ B_3 &= \frac{2[1 + 8G(G-1) + \alpha^2]}{(2G-1)^2(1+\alpha^2)}, \end{aligned} \tag{22}$$

respectively. To find the smallest value between B_1, B_2, and B_3, we should obtain their extreme points when the value of α is fixed. Thus, the smallest values of B_2 and B_3 can be obtained:

$$\begin{aligned} (B_2)_{\min} &= \lim_{\alpha\to 0} \frac{2 + 2[1 + 8G(G-1)]\alpha^2}{(2G-1)^2(1+\alpha^2)} = \frac{2}{(2G-1)^2}, \\ (B_3)_{\min} &= \lim_{\alpha\to \infty} \frac{2[1 + 8G(G-1) + \alpha^2]}{(2G-1)^2(1+\alpha^2)} = \frac{2}{(2G-1)^2}. \end{aligned} \tag{23}$$

As Equation (23) shows, the value of B_2 in the limit of $\alpha = 0$ is equivalent to the one of B_3 in the limit of $\alpha = \infty$, and this is because under both two conditions, three-mode entanglement will reduce to two-mode entanglement only pumped by one pump beam; thus, $(B_2)_{\min}$ and $(B_3)_{\min}$ cannot be viewed as the boundary of three-mode entanglement. The other effective boundary B_1 (trace B) is depicted in Figure 6b, and its value is always larger than the one of V_{s12}^{opt} (trace A); thus, genuine three-mode entanglement is present in the whole gain range. Thus, the optimal single-condition criterion can be used to quantify genuine three-mode entanglement more efficiently than the single-condition criterion.

3.3. PPT Criterion

Finally, the PPT criterion can also be used to quantify genuine three-mode entanglement [18,19,23]. For three-mode entanglement, the three possible 1×2 partitions ($\hat{a}_s - (\hat{a}_1, \hat{a}_2)$, $\hat{a}_1 - (\hat{a}_s, \hat{a}_2)$, and $\hat{a}_2 - (\hat{a}_s, \hat{a}_1)$) have to be tested. When the smallest symplectic eigenvalue for each of the three PT CMs is smaller than 1, all the partitions are inseparable, and genuine three-mode entanglement will exist.

When the PT operation is applied to the mode $\hat{a}_s$, the entanglement between $\hat{a}_s$ and the rest of the modes ($\hat{a}_1$ and $\hat{a}_2$) can be quantified by the smallest symplectic eigenvalue T_{s-12}:

$$T_{s-12} = \frac{\sqrt{1 + 3\alpha^2 + 3\alpha^4 + \alpha^6 - 8G(1+\alpha^2)^3 + 8G^2(1+\alpha^2)^3 - 4(2G-1)(1+\alpha^2)^3\sqrt{G(G-1)}}}{(1+\alpha^2)^{3/2}}. \tag{24}$$

As depicted in Figure 7a, the value of T_{s-12} in the whole region is smaller than 1, meaning that the mode $\hat{a}_s$ is quantum entangled with the rest of the modes ($\hat{a}_1$ and $\hat{a}_2$). It should be emphasized that the value of T_{s-12} is independent of the interaction strength ratio α, and this is because the combination of the two idler modes $\hat{a}_1$ and $\hat{a}_2$ can be viewed as a combined idler mode. Similarly, when the PT operation is applied to the modes $\hat{a}_1$ and $\hat{a}_2$, the smallest symplectic eigenvalues are T_{1-s2} and T_{2-s1}, and their detailed results can be written as

$$T_{1-s2} = \frac{\sqrt{\begin{array}{c} 1 + (8G-5)\alpha^2 + (8G^2-5)\alpha^4 + [1 + 8G(G-1)]\alpha^6 \\ -4[(2G-1)\alpha^2 - 1](\alpha + \alpha^3)\sqrt{(G-1)(1+G\alpha^2)} \end{array}}}{(1+\alpha^2)^{3/2}}, \tag{25}$$

and

$$T_{2-s1} = \frac{\sqrt{\begin{array}{c}1-5\alpha^2-5\alpha^4+\alpha^6+8G^2(1+\alpha^2)+8G(\alpha^4-1)\\ -4(\alpha^2+1)(2G-1+\alpha^2)\sqrt{(G-1)(G+\alpha^2)}\end{array}}}{(1+\alpha^2)^{3/2}}, \tag{26}$$

respectively. The contour plots of T_{1-s2} and T_{2-s1} are depicted in Figure 7b,c, respectively. It can be clearly seen that the values of T_{1-s2} and T_{2-s1} are both smaller than 1 in the whole parametric region, showing that the three partitions are all inseparable and the existence of genuine three-mode entanglement in the whole parameter region.

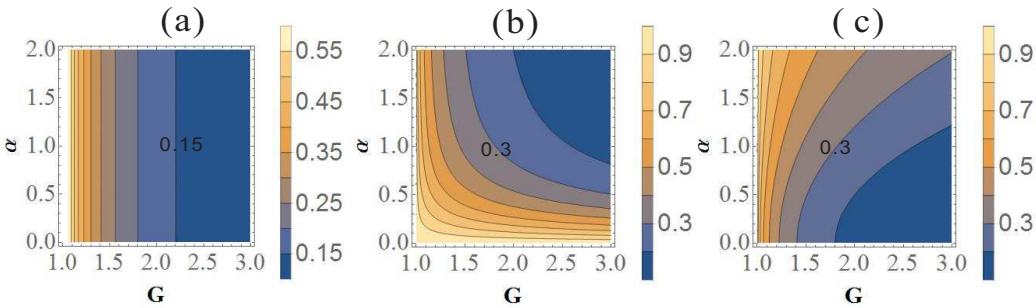

Figure 7. The dependence of (**a**) T_{s-12}; (**b**) T_{1-s2}; and (**c**) T_{2-s1}.

4. Conclusions

In conclusion, we theoretically predicted that the concurrent parametric amplifier as a simple system can be used to generate two-mode and three-mode entanglement. The Duan criterion and PPT criterion can be used to quantify two-mode entanglement, which is present in the two pairs. The two-condition and optimal single-condition criterion were both analyzed to search for the entanglement region. In the case of the optimal single-condition criterion, genuine three-mode entanglement is present in the whole parameter region. More importantly, the PPT criterion was also used to claim the existence of genuine three-mode entanglement in the whole parameter region. Our concurrent parametric amplifier for generating multi-mode correlation and entanglement is integrated and phase-insensitive.

Author Contributions: H.W. contributed to the development of the conceptualization, the discussions of the results, and the comments on the manuscript. Y.S. contributed to the validation, investigation, and data curation on the manuscript. All authors have read and agreed to the published version of the manuscript.

Funding: This research was funded by the Zhejiang Provincial Natural Science Foundation of China (LY22A040007), the National Natural Science Foundation of China (11804323), and the Fundamental Research Funds for the Provincial Universities of Zhejiang (2021YW29).

Conflicts of Interest: The authors declare no conflict of interest.

References

1. Carman, R.L.; Chiao, R.Y.; Kelley, P.L. Observation of Degenerate Stimulated Four-Photon Interaction and Four-Wave Parametric Amplification. *Phys. Rev. Lett.* **1966**, *17*, 1281–1283. [CrossRef]
2. Slusher, R.E.; Hollberg, L.W.; Yurke, B.; Mertz, J.C.; Valley, J.F. Observation of Squeezed States Generated by Four-Wave Mixing in an Optical Cavity. *Phys. Rev. Lett.* **1985**, *55*, 2409–2412. [CrossRef]
3. Liu, Y.; Huo, N.; Li, J.; Li, X. Long-distance distribution of the telecom band intensity difference squeezing generated in a fiber optical parametric amplifier. *Opt. Lett.* **2018**, *43*, 5559–5562. [CrossRef]
4. McCormick, C.F.; Boyer, V.; Arimondo, E.; Lett, P.D. Strong Relative Intensity Squeezing by Four-Wave Mixing in Rubidium Vapor. *Opt. Lett.* **2007**, *33*, 178–180. [CrossRef]
5. Boyer, V.; Marino, A.M.; Pooser, R.C.; Lett, P.D. Entangled Images from Four-Wave Mixing. *Science* **2008**, *321*, 544–547. [CrossRef]
6. Marino, A.M.; Pooser, R.C.; Boyer, V.; Lett, P.D. Tunable Delay of Einstein-Podolsky-Rosen Entanglement. *Nature* **2009**, *457*, 859–862. [CrossRef]

7. Pooser, R.C.; Marino, A.M.; Boyer, V.; Jones, K.M.; Lett, P.D. Low-Noise Amplification of a Continuous-Variable Quantum State. *Phys. Rev. Lett.* **2009**, *103*, 010501. [CrossRef]
8. Jing, J.; Liu, C.; Zhou, Z.; Ou, Z.Y.; Zhang, W. Realization of a Nonlinear Interferometer with Parametric Amplifiers. *Appl. Phys. Lett.* **2011**, *99*, 011110. [CrossRef]
9. Hudelist, F.; Kong, J.; Liu, C.; Jing, J.; Ou, Z.Y.; Zhang, W. Quantum Metrology with Parametric Amplifier-Based Photon Correlation Interferometers. *Nat. Commun.* **2014**, *5*, 3049. [CrossRef]
10. Qin, Z.; Cao, L.; Wang, H.; Marino, A.M.; Zhang, W.; Jing, J. Experimental Generation of Multiple Quantum Correlated Beams from Hot Rubidium Vapor. *Phys. Rev. Lett.* **2014**, *113*, 023602. [CrossRef]
11. Fang, Y.; Jing, J. Quantum Squeezing and Entanglement from a Two-Mode Phase-Sensitive Amplifier via Four-Wave Mixing in Rubidium Vapor. *New J. Phys.* **2015**, *17*, 023027. [CrossRef]
12. Fang, Y.; Feng, J.; Cao, L.; Wang, Y.; Jing, J. Experimental Implementation of a Nonlinear Beamsplitter Based on a Phase-Sensitive Parametric Amplifier. *Appl. Phys. Lett.* **2016**, *108*, 131106. [CrossRef]
13. Wu, M.C.; Schmittberger, B.L.; Brewer, N.R.; Speirs, R.W.; Jones, K.M.; Lett, P.D. Twin-beam intensity-difference squeezing below 10 Hz. *Opt. Express* **2019**, *27*, 4769–4780. [CrossRef]
14. Corzo, N.V.; Marino, A.M.; Jones, K.M.; Lett, P.D. Noiseless Optical Amplifier Operating on Hundreds of Spatial Modes. *Phys. Rev. Lett.* **2012**, *109*, 043602. [CrossRef]
15. Boyer, V.; Marino, A.M.; Lett, P.D. Generation of Spatially Broadband Twin Beams for Quantum Imaging. *Phys. Rev. Lett.* **2008**, *100*, 143601. [CrossRef]
16. Daems, D.; Bernard, F.; Cerf, N.J.; Kolobov, M.I. Tripartite entanglement in parametric down-conversion with spatially structured pump. *J. Opt. Soc. Am. B* **2010**, *27*, 447–451. [CrossRef]
17. Duan, L.M.; Giedke, G.; Cirac, J.I.; Zoller, P. Inseparability Criterion for Continuous Variable Systems. *Phys. Rev. Lett.* **2000**, *84*, 2722–2725. [CrossRef]
18. Simon, R. Peres-Horodecki Separability Criterion for Continuous Variable Systems. *Phys. Rev. Lett.* **2000**, *84*, 2726–2729. [CrossRef]
19. Werner, R.F.; Wolf, M.M. Bound Entangled Gaussian States. *Phys. Rev. Lett.* **2001**, *86*, 3658–3661. [CrossRef]
20. Barbosa, F.A.S.; de Faria, A.J.; Coelho, A.S.; Cassemiro, K.N.; Villar, A.S.; Nussenzveig, P.; Martinelli, M. Disentanglement in Bipartite Continuous-Variable Systems. *Phys. Rev. A* **2011**, *84*, 052330. [CrossRef]
21. Barbosa, F.A.S.; Coelho, A.S.; de Faria, A.J.; Cassemiro, K.N.; Villar, A.S.; Nussenzveig, P.; Martinelli, M. Robustness of bipartite Gaussian entangled beams propagating in lossy channels. *Nat. Photonics* **2010**, *4*, 858–861. [CrossRef]
22. Loock, P.V.; Furusawa, A. Detecting genuine multipartite continuous-variable entanglement. *Phys. Rev. A* **2003**, *67*, 052315. [CrossRef]
23. Coelho, A.S.; Barbosa, F.A.S.; Cassemiro, K.N.; Villar, A.S.; Martinelli, M.; Nussenzveig, P. Three-Color Entanglement. *Science* **2009**, *326*, 823–826. [CrossRef]